International Journal of Minerals, Metallurgy and Materials
Volume 18, Number 2, April 2011, Page 178
DOI: 10.1007/s12613-201-0419-0

Passivation process of X80 pipeline steel in bicarbonate solutions

Jian-long Zhou[1)], *Xiao-gang Li*[1)], *Cui-wei Du*[1)], *Ying Pan*[2)], *Tao Li* [3)], *and Qian Liu*[1)]

1) School of Materials Science and Engineering, University of Science and Technology Beijing, Beijing 100083, China
2) Wuhan Research Institute of Materials Protection, Wuhan 430030, China
3) School of Materials & Metallurgy, Inner Mongolia University of Science and Technology, Baotou 014010, China
(Received: 21 April 2010; revised: 9 June 2010; accepted: 13 July 2010)

Abstract: The passivation process of X80 pipeline steel in bicarbonate solutions was investigated using potentiodynamic, dynamic electrochemical impedance spectroscopy (DEIS), and Mott-Schottky measurements. The results show that the shape of polarization curves changes with HCO_3^- concentration. The critical 'passive' concentration is 0.009 mol/L HCO_3^- for X80 pipeline steel in bicarbonate solutions. No anodic current peak exists in HCO_3^- solutions when the concentration is lower than 0.009 mol/L, whereas there are one and two anodic current peaks when the HCO_3^- concentration ranges from 0.009 to 0.05 mol/L and is higher than 0.1 mol/L, respectively. DEIS measurements show that there exist active dissolution range, transition range, pre-passive range, passive layer formation range, passive range, and trans-passive range for X80 pipeline steel in the 0.1 mol/L HCO_3^- solutions. The results of DEIS measurements are in complete agreement with the potentiodynamic diagram. An equivalent circuit containing three sub-layers is used to explain the Nyquist plots in the passive range. Analyses are well made for explaining the corresponding fitted capacitance and impedance. The Mott-Schottky plots show that the passive film of X80 pipeline steel is an n-type semiconductor, and capacitance measurements are in good accordance with the results of DEIS experiment.

Keywords: pipeline steel; bicarbonate solutions; passivation; potentiodynamic polarization; electrochemical impedance spectroscopy

[*This work was financially supported by the National Science and Technology Infrastructure Platforms Construction Projects (No.2005DKA10400).*]

1. Introduction

X80 steel, known as a micro-alloyed mild steel, is preferred to be used in buried natural gas pipelines due to its good weldability, high strength, and good ductility [1]. Its corrosion performance is a key problem for life expectancy, especially in a soil environment.

Bicarbonate is one of the main substances in various soil environments affecting the corrosion behavior of pipeline steels [2-3]. According to previous studes [4-5], HCO_3^- ions have multiple effects on anodic reactions of iron, such as participating anodic dissolution through active adsorption, inhibiting further anodic dissolution by forming a protective film, and enhancing anodic dissolution through dissolving the protective film.

To make clear the detailed mechanisms of HCO_3^- ions on iron, researchers have made a series of investigations from different angles. Zeng *et al*. [6] studied the passive film on X70 pipeline steel in a 0.5 mol/L HCO_3^- solution and found that the addition of HCO_3^- was beneficial to both the formation of the passive film and the inhibition of the pitting of X70 micro-alloyed steel.

Hancock and Gilroy *et al*. [7-8] studied the passivation

Corresponding author: Xiao-gang Li E-mail: lixiaogang99@263.net

characteristics of iron in carbonate solutions with a galvanostatic method and observed two arrests in potential. The initial arrest was ascribed to the formation of the film consisting of ferrous carbonate and hydroxide, and the second to the oxidation of the former film to ferric oxide.

Thomas *et al*. [9] found two distinct current maxima in the polarization curve for iron in carbonate solutions. The initial oxidation peak was attributed to the formation of a film, which mainly consisted of an oxide of iron, probably magnetite, or ferrous carbonate. The second oxidation peak was thought to be related to the oxidation of ferrous carbonate present in the film to γ-ferric oxide.

Lu *et al.* [4] found that the anodic polarization curves of Fe in 0.01–1.0 mol/L HCO_3^- solutions showed a typical active-passive-transpassive characteristic, and the number of anodic current peaks varied with HCO_3^- concentration.

Mao *et al.* [10] indicated that pitting corrosion may be the first step for pipeline fracture in a bicarbonate environment. Whether pits could be formed or not was relevant with the HCO_3^- concentration.

However, most studies mainly focus on the properties of the passive film itself. There have been very few attempts to investigate the anodic electrochemical behaviors, such as the passivation process of iron and carbon steels, especially pipeline steels in solutions containing HCO_3^-. Therefore, the present study focuses on the investigation of the passivation process of X80 pipeline steel in HCO_3^- solutions to have a better understanding of its corrosion mechanisms.

2. Experimental

2.1. Materials and solutions

X80 pipeline steel samples were used as working electrodes. Samples were cut into 10 mm×10 mm coupons for electrochemical measurements. The samples were spot-welded to copper wires for electrical contact. Insulation of the samples was provided by epoxy resin. Prior to measurements, the specimens were ground mechanically with emery papers up to 1500 grit and then rinsed with deionized water and ethanol successively.

The test solutions were $NaHCO_3$ with different concentrations, and the pH value for all the solutions is approximately 8.31. All solutions were prepared with deionized water and analytical grade $NaHCO_3$ reagent.

2.2. Electrochemical measurements

Potentiodynamic, dynamic electrochemical impedance spectroscopy (DEIS), and Mott-Schottky measurements were carried out on Model VMP3 instrument from Princeton Applied Research in this paper. All the electrochemical experiments were performed in a conventional three-electrode cell system, in which a saturated calomel electrode (SCE) was used as the reference electrode and a platinum sheet as the counter electrode. Unless otherwise stated in this paper, all potentials quoted were referred to SCE. In all the electrochemical measurements, the specimens were first cathodically polarized at –1.3 V for 5 min and then stabilized for 0.5 h.

In potentiodynamic measurements, the polarization curves were obtained ranging from –0.25 V (*vs*. open circuit potential (OCP)) to 1.40 V at a potential scanning rate of 1 mV/s.

In DEIS measurements, the potential was scanned from –0.74 to 1.26 V at a potential scanning rate of 0.02 V per cycle. A total of 100 cycles were performed in the whole test. The amplitude of the perturbation signal was 10 mV, and the test frequencies ranged from 5 kHz to 1 Hz. ZSimpWin software was used for data fitting.

To obtain Mott-Schottky plots for each passive film at different film formation potentials, the specimens were pre-passivated at film formation potentials for 2 h, and then the potential was scanned from –0.20 to 0.80 V in the anodic direction. An AC signal with an amplitude of 10 mV and a frequency of 1000 Hz were superimposed on the scanning signal.

3. Results and discussion

3.1. Effects of HCO_3^- concentration on polarization characteristics

Fig. 1 illustrates the potentiodynamic polarization curves of X80 pipeline steel samples in $NaHCO_3$ solutions of various concentrations. The shape of polarization curves changes with HCO_3^- concentration.

When the HCO_3^- concentration increases from 0.001 to 0.008 mol/L, the anodic reaction is controlled by an active process. The corrosion current density increases gradually when the polarization potential is lower than 0.75 V, indicating that the corrosion of X80 pipeline steel is accelerated at low potential in HCO_3^- solutions with low concentration. When the polarization potential is higher than 0.75 V, the anodic current density in 0.008 mol/L HCO_3^- solution is lower than that in 0.005 mol/L, which reveals that very weak ‘passivity’ phenomenon has appeared.

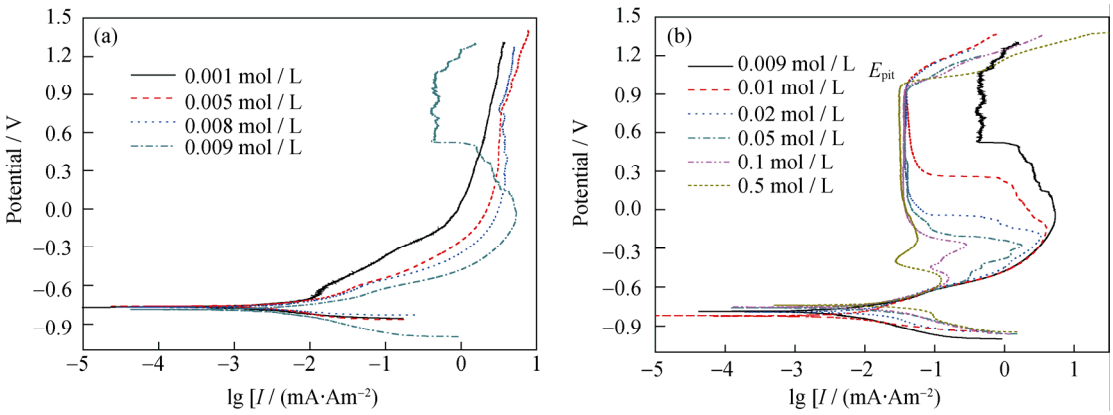

Fig. 1. Potentiodynamic diagram of X80 pipeline steel in various HCO_3^- solutions at a potential scanning rate of 1 mV/s.

When the HCO_3^- concentration is 0.009 mol/L, the anodic current density increases with increasing polarization potential at relatively low potential. However, when the polarization potential is higher than –0.15 V, the anodic current decreases gradually, and it is lower than that at 0.001 mol/L when the polarization potential is higher than 0.40 V, revealing that an anodic peak will be formed in the 0.009 mol/L HCO_3^- solution. Moreover, a weak 'passive' region is observed at the potential between approximate 0.50 and 1.05 V.

With the HCO_3^- concentration further increasing to 0.01, 0.02, and 0.05 mol/L, only one anodic current peak can be observed, and the anodic current peak becomes much sharper, but the maximum current density decreases gradually. Meanwhile, with the increase of HCO_3^- concentration, the polarization potential at the anodic peak moves to a lower value, the passive potential range becomes wider and is kept at about 1.00 V, and the passive current density is lowered and kept stable gradually. Therefore, it is much easier for X80 pipeline steel to passivate at relatively high HCO_3^- concentration. Furthermore, the pitting potential (E_{pit}) is a little lower at higher HCO_3^- concentrations, indicating that the pitting propagation of X80 pipeline steel is faster in the trans-passive region with increasing HCO_3^- concentration.

When the HCO_3^- concentration reaches 0.1 mol/L, two apparent anodic current peaks can be observed, and the corrosion current density at the peak decreases greatly. Furthermore, when the HCO_3^- concentration increases to 0.5 mol/L, the second anodic current peak is much lower than that in the 0.1 mol/L HCO_3^- solution, but no obvious change can be observed for the primary anodic current peak. Similar to the phenomenon in the 0.1 mol/L HCO_3^- solution, the passive region is quite stable. It is worth noting that negative current exists in the 0.5 mol/L HCO_3^- solution, which may be due to the reduction of oxygen adsorbed on the electrode surface [11].

Therefore, the number of anodic current peaks varies with HCO_3^- concentrations. In the range of OCP to E_{pit}, the corrosion rate of X80 pipeline steel increases at first and then decreases. Besides, with the increase of HCO_3^- concentration, the turnng point potential decreases. The critical 'passive' concentration is 0.009 mol/L HCO_3^-, indicating that ionic conduction is the dominant factor when the HCO_3^- concentration is lower than that. When the HCO_3^- concentration further increases, HCO_3^- anions become beneficial to passivation of X80 pipeline steel. The anodic current density peak is narrower, and the value of the current density peak is lower. Meanwhile, the passivation region becomes wider, and the passive current density turns to be smaller and stable. When the HCO_3^- concentration reaches 0.1 mol/L or higher, two obvious anodic current peaks exist, but the anodic current density of both the peaks decreases sharply. For X80 pipeline steel, more stable pitting corrosion is ready to occur once the polarization potential is higher than E_{pit} with increasing HCO_3^- concentration.

3.2. Effect of polarization potential on DEIS

DEIS is an appropriate method for impedance measurements of pitting corrosion [12]. To make a better understanding of DEIS results, a potentiodynamic diagram of X80 pipeline steel in the 0.1 mol/L HCO_3^- solution with a potential scanning rate of 1 mV/s is illustrated in Fig. 2. A DEIS diagram of X80 pipeline steel in the 0.1 mol/L HCO_3^- solution from –0.74 to 1.26 V is shown in Fig. 3.

According to the anodic polarization curve in Fig. 2, there are two obvious anodic current peaks, a current valley, and a passive region. The ranges *AB*, *BC*, *CD*, *DE*, *EF*, and *FG* can be categorized as active dissolution range, transition range, pre-passive range, passive layer formation range, passive range, and trans-passive range, correspondingly.

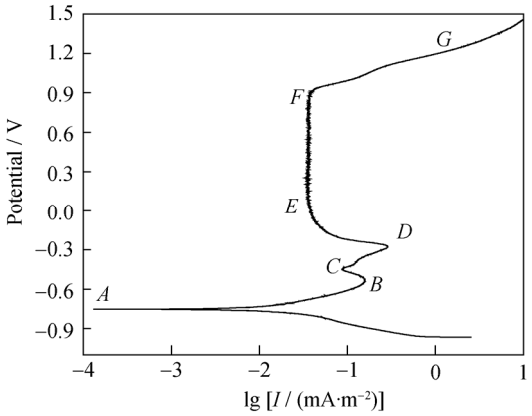

Fig. 2. Potentiodynamic diagram of X80 pipeline steel in the 0.1 mol/L HCO_3^- solution.

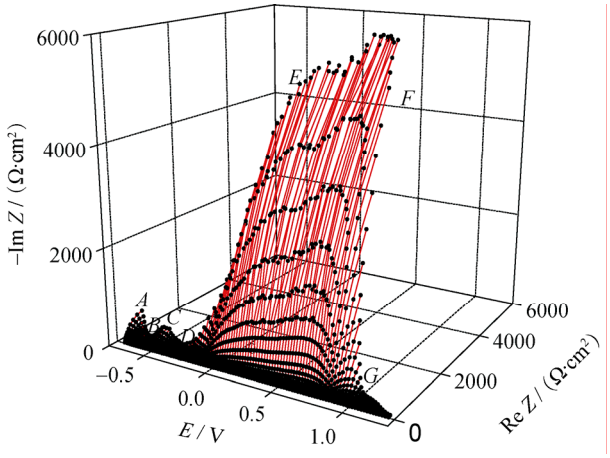

Fig. 3. DEIS diagram of X80 pipeline steel in the 0.1 mol/L HCO_3^- solution.

According to the DEIS curves in Fig. 3, there are two impedance valleys, an impedance peak, and an impedance plateau. As the impedance is in the inverse ratio of current density, the impedance valley corresponds to the current peak, and the impedance peak corresponds to the current valley. Therefore, with the increase of polarization potential, the sequential impedance changes for X80 pipeline steel are as follows: decreasing in range *AB*, increasing in range *BC*, decreasing in range *CD*, increasing sharply in range *DE*, relatively stable in range *EF*, and decreasing sharply in range *FG*. From DEIS diagram, it can also be seen that the impedance at point *D* is lower than that at point *B*, which reveals a larger current density at point *D*. In addition, the impedance in range *EF* is very large, indicating the passive state of the surface of X80 pipeline steel. When the potential is higher than point *F*, pitting occurs. Compared with the current variation in Fig. 2, the DEIS diagram is completely in agreement with the potentiodynamic diagram. Moreover, the Nyquist plots shown in Fig. 3 can represent the impedance characteristics at various potentials, which is beneficial to the mechanism study of the corrosion process of X80 pipeline steel in HCO_3^- solutions. The details of each equivalent Nyquist plot are illustrated in Fig. 4.

As shown in Figs. 4(a)-(d), in the 0.1 mol/L HCO_3^- solution, a series of the depressed semicircles reflecting the capacitance property can be observed for X80 pipeline steel when the polarization potential is below 0 V. However, when the polarization potential is between 0 V and 0.74 V, the diffusive characteristics of impedance can be observed in the range of low frequency, as shown in Fig. 4(e). As the polarization potential further increases to over 0.96 V, the depressed semicircles appear again, which are shown in Fig. 4(f).

Corresponding to range *AB* in Fig. 3, the Nyquist plots in Fig. 4(a) show that the diameter of the depressed semicircles decreases with the polarization potential increasing from –0.74 to –0.60 V, indicating the increased tendency of current density at the first stage, which is associated with the active dissolution of Fe [3]. It can be written as Eq. (1).

$$Fe \rightarrow Fe^{2+} + 2e \quad (1)$$

When increasing the polarization potential from –0.60 to –0.48 V, the diameter of the depressed semicircles increases, as shown in Fig. 4(b), indicating the decreased tendency of current density, which may be associated with the formation of a protective film of $FeCO_3$ or $Fe(OH)_2$ [3]. The process corresponds to range *BC* in Fig. 3. The reaction can be written as Eq. (2) or (3).

$$Fe + HCO_3^- \rightarrow FeCO_3 + H^+ + 2e \quad (2)$$

$$Fe + 2H_2O \rightarrow Fe(OH)_2 + 2H^+ + 2e \quad (3)$$

When the HCO_3^- concentration is relatively high and the OH^- concentration is rather low, according to calculation results of Nernst equation, $FeCO_3$ should be a primary component of the protective film.

Fig. 4(c) shows the similar capacitive variation to Fig. 4(a) when further increasing the polarization potential from –0.48 to –0.28 V. This stage corresponds to range *CD* in Fig. 3. The increased tendency of current density at this stage may relate to the active dissolution of $FeCO_3$ [13]. It can be expressed by Eqs. (4) and (5):

$$FeCO_3 + HCO_3^- \rightarrow Fe(CO_3)_2^{2-} + H^+ \quad (4)$$

$$FeCO_3 + H^+ \rightarrow Fe^{2+} + HCO_3^- \quad (5)$$

Similar to Fig. 4(b), Fig. 4(d) shows the capacitive variation when the polarization potential increases between –0.28 and 0 V. This stage corresponds to range *DE* in Fig. 3. The sharp increase of capacitive diameter represents the drastic decrease of current density at this stage, which may be relevant

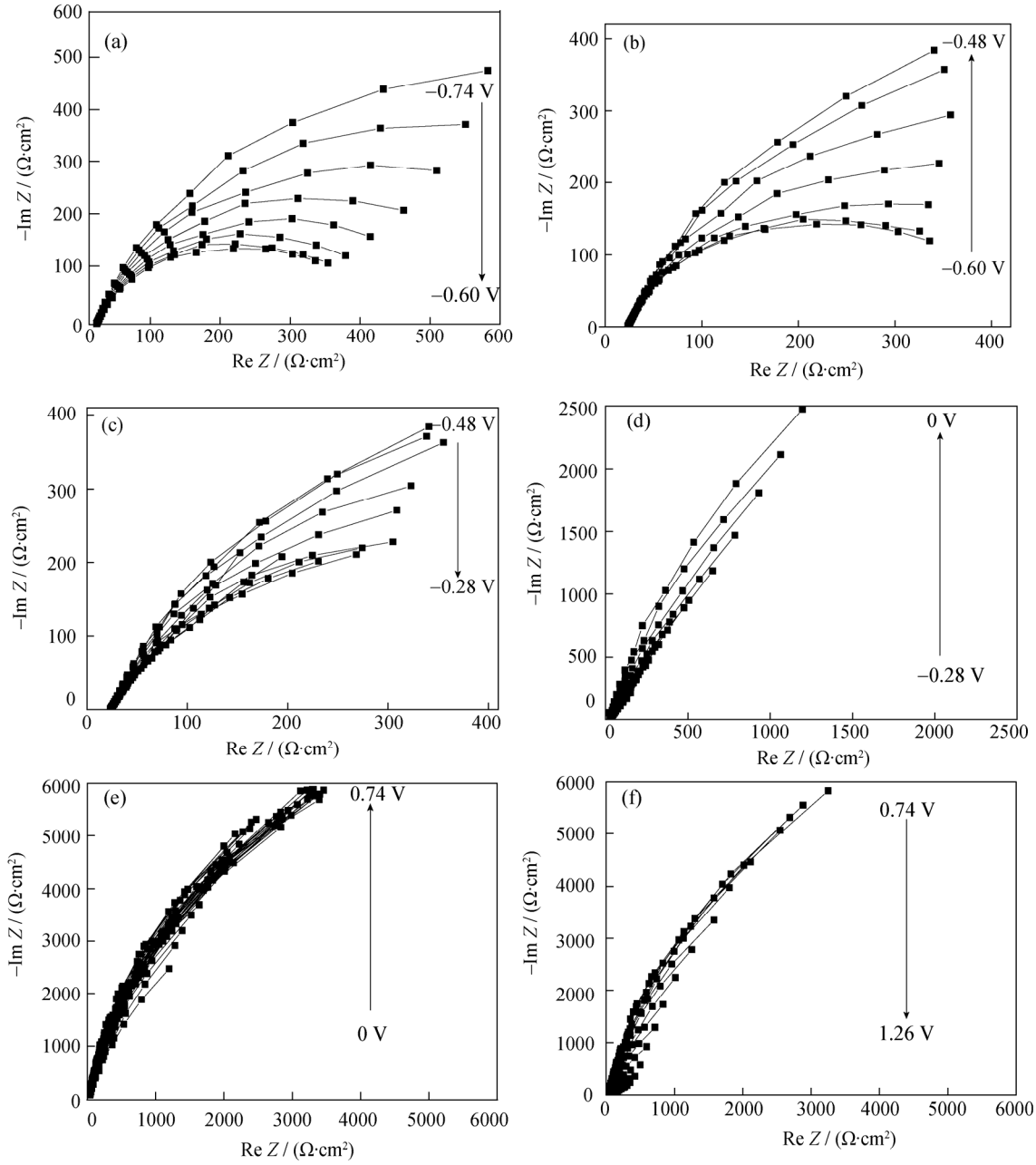

Fig. 4. Equivalent Nyquist plots of X80 pipeline steel in the 0.1 mol/L HCO_3^- solution at various potentials in Fig. 3: (a)–0.74- –0.60 V; (b) –0.60- –0.48 V; (c) –0.48- –0.28 V; (d) –0.28-0 V; (e) 0-0.74 V; (f) 0.74-1.26 V.

to the formation of a protective film of $FeCO_3$, Fe_3O_4, and γ-Fe_2O_3. It can be expressed by Eqs. (2), (6) and (7), (8), respectively.

$$3FeCO_3 + 5OH^- \rightarrow Fe_3O_4 + 3HCO_3^- + H_2O + 2e \quad (6)$$

$$Fe + 2Fe(OH)_2 + 4OH^- \rightarrow Fe_3O_4 + 4H_2O + 4e \quad (7)$$

$$2Fe_3O_4 + H_2O \rightarrow 3\gamma\text{-}Fe_2O_3 + 2H^+ + 2e \quad (8)$$

Therefore, the corrosion of X80 pipeline steel is greatly inhibited.

When the polarization potential increases from 0 V to 0.74 V, the convective diffusion impedance is observed in the range of low frequency. At this stage, the stable protective films of $FeCO_3$, Fe_3O_4, and γ-Fe_2O_3 are formed and kept. However, with the increase of the polarization potential, there is a conversion from $FeCO_3$ to Fe_3O_4 and more stable γ-Fe_2O_3.

When further increasing the polarization potential from 0.74 to 1.26 V, the capacitive property of the Nyquist plots can be observed. The diameter of the capacitive loop decreases at this stage, and pitting corrosion occurs at the polarization potential higher than 0.96 V. The reaction at this

stage can be expressed by Eq. (9).

$$Fe + 4OH^- \rightarrow FeO_4^{2-} + 4H^+ + 6e \quad (9)$$

From above analysis, the EIS diagrams in Fig. 4 are in good agreement with the results of the polarization curve in Fig. 2. However, it should also be noticed that the maximum diameter of the capacitive loop is at the potential approximately 0.74 V; thus, it can be thought as the transition region from passive state to active state between 0.74 V and 0.96 V.

Studying the passive property is of great significance to understand the corrosion characteristics of materials. According to Ref. [14], the total impedance of a passive layer is a sum of three parts. The first part concerns the passive layer/metal interface; the second part is related to the volume properties of the passive layer; and the third part describes the passive layer/electrolyte interface. In many cases, the impedances of the passive layer/metal and passive layer/electrolyte interfaces can be neglected with respect to the volume impedance of the passive layer. In this system, three different passive products are formed on the surface of the electrode; thus, an equivalent circuit containing three sub-layers is used to explain the experimental spectra for X80 pipeline steel in the 0.1 mol/L HCO_3^- solution as shown in Fig. 5.

The equivalent circuit is in good agreement with the Nyquist plots in the passive range. Moreover, the resultant capacitance and impedance of each sub-layer are shown in Fig. 6.

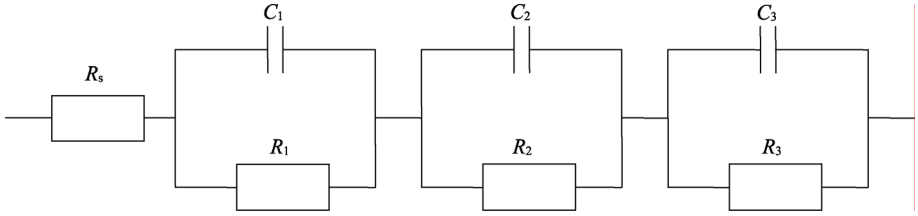

Fig. 5. Equivalent circuit of X80 pipeline steel describing the passive layer: R_s—solution impedance; C_1, C_2, and C_3—capacitances of the inner, intermediate, and outer sub-layers, respectively; R_1, R_2, and R_3—impedances of the inner, intermediate, and outer sub-layers, respectively.

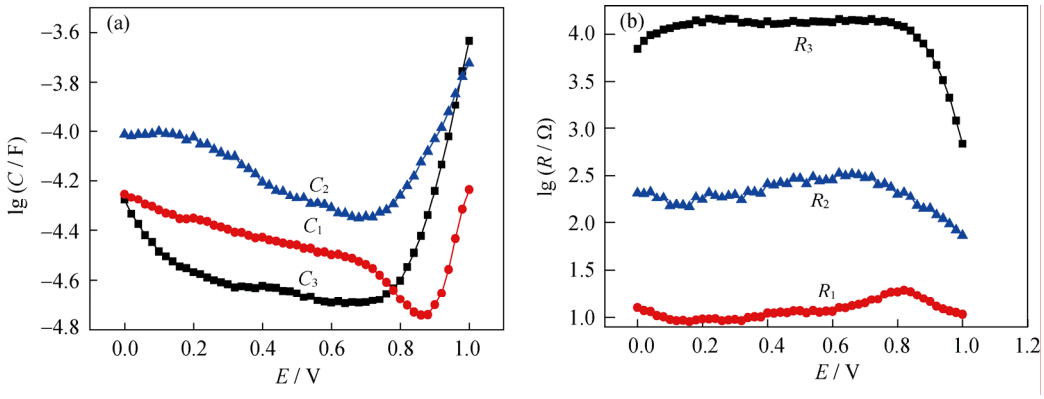

Fig. 6. Capacitance (a) and impedance (b) of each sub-layer in the 0.1 mol/L HCO_3^- solution.

As can be seen from Fig. 6(a), an increase in the polarization potential in the anodic direction causes a decrease in the three sub-layer capacities. In the polarization potential range of 0-0.95 V, the intermediate sub-layer has the highest capacity, while the outer one has the lowest capacity. However, as shown in Fig. 6(b), the sequence of impedance from high to low is the outer sub-layer, intermediate sub-layer, and inner sub-layer. According to aforementioned discussion, the passive layer consists of $FeCO_3$ (inner layer), Fe_3O_4 (intermediate layer) and γ-Fe_2O_3 (outer layer). As $FeCO_3$ and γ-Fe_2O_3 have poor conductivity whereas Fe_3O_4 has rather good conductivity [11], therefore, it can be concluded that the thickness of the inner sub-layer is thinner than that of both the intermediate sub-layer and the outer sub-layer. With increasing the polarization the potential from 0 to 0.74 V, the slight increase of impedance in all the three sub-layers reveals the increase of film thickness in the passive range. However, when a more noble polarization potential approximate to the pitting potential is applied, the capacitances increase sharply, revealing that the film has suffered from attack. On the contrary, the impedance decreases greatly. The above result is in good agreement with the DEIS diagram.

3.3. Semi-conductor properties of the passive films

To further investigate the semi-conductive properties of the passive region, Fig. 7 illustrates the Mott-Schottky plots of X80 pipeline steel specimens at different potentials for 2 h in the 0.1 mol/L HCO_3^- solution.

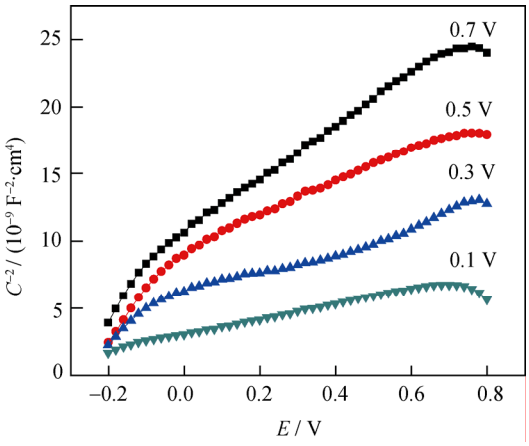

Fig. 7. Mott-Schottky plots of the passive film at different potentials for 2 h.

As can be observed in Fig. 7, C^{-2} shows linear increase behavior with increasing polarization potential at the various film formation potentials of the passive film for X80 pipeline steel, which is in consistent with the theoretical calculation described in another literature [15]. In good agreement with the decreased tendency of capacitance measurements with increasing polarization potential in the DEIS experiment, the slopes of Mott-Schottky plots are positive, indicating that the passive film is an n-type semiconductor. Moreover, the increase of C^{-2} with enhancing film formation potential reveals the increase of film thickness. Furthermore, the turning point of the capacitance value is at approximately 0.74 V, which is also in accordance with the maximum impedance result shown in DEIS measurements. Therefore, the thickness of the passive film becomes thicker with increasing the polarization potential to 0.74 V, and then it decreases due to the increase of anodic current density.

4. Conclusions

(1) The potentiodynamic diagram reveals that the shape of polarization curves changes with HCO_3^- concentration. The 0.009 mol/L HCO_3^- is the critical 'passive' concentration. With increasing HCO_3^- concentration, the passive potential range becomes wider, whereas the anodic current peak appears narrower and the peak value gets lower.

(2) The DEIS technique is a good tool for measuring the dynamic variation of each Nyquist plot, the results of which are in complete accordance with that of potentiodynamic measurements. The corrosion products change with polarization potential, and an equivalent circuit containing three sub-layers can well explain the experimental spectra of X80 pipeline steel in the passive range.

(3) The Mott-Schottky plots show that the thickness of the passive film tends to increase with the increase of polarization potential to 0.74 V, and then it tends to decrease due to the enhancement of anodic current density. The Mott-Schottky results are in good accordance with DEIS measurements.

References

[1] P. Liang, C.W. Du, X.G. Li, *et al*., Effect of hydrogen on the stress corrosion cracking behavior of X80 pipeline steel in Ku'erle soil simulated solution, *Int. J. Miner. Metall. Mater*., 16(2009), No.4, p.407.

[2] M.C. Li and Y.F. Cheng, Corrosion of the stressed pipe steel in carbonate-bicarbonate solution studied by scanning localized electrochemical impedance spectroscopy, *Electrochim. Acta*, 53(2008), p.2831

[3] C.W. Du, X.G. Li, X. Chen, *et al*. Crevice corrosion behavior of X70 steel in HCO_3^- solution under cathodic polarization, *Acta Metall. Sin. Engl. Lett.*, 21(2008), p.235.

[4] Z.P. Lu, C.B. Huang, and D.L. Huang, Effects of a magnetic field on the anodic dissolution, passivation and transpassivation behaviour of iron in weakly alkaline solutions with or without halides, *Corros. Sci*., 48(2006), p.3049.

[5] P. Liang, X.G. Li, C.W. Du, *et al*., Influence of chloride ions on the corrosion resistance of X80 pipeline steel in $NaHCO_3$ solution, *J. Univ. Sci. Technol. Beijing* (in Chinese), 30(2008), No.7, p.735.

[6] Y.M. Zeng, J.L. Luo, and P.R. Norton, Initiation and propagation of pitting and crevice corrosion of hydrogen-containing passive films on X70 micro-alloyed steel, *Electrochim. Acta*, 49(2004), p.703.

[7] P. Hancock, and J.E.O. Mayne, The inhibition of the corrosion of iron in the neutral and alkaline solutions, *J. Appl. Chem*., 9(1959), p.345.

[8] B. Gilroy and J.E.O. Mayne, The inhibition of the corrosion of iron in alkaline solutions, *Br. Corros. J*., 1(1966), p.161.

[9] J.G.H. Thomas, T.J. Nurse, and R. Walker, Anodic passivation of iron in carbonate solutions, *Br. Corros. J.*, 5(1970), p.87.

[10] X. Mao, X. Liu, and R.W. Revie, Pitting corrosion of pipeline steel in dilute bicarbonate solution with chloride ions, *Corrosion*, 50(1994), No. 9, p.651.

[11] J.A. von Fraunhofer, The polarization behaviour of mild steel in aerated and de-aerated 1M $NaHCO_3$ solution, *Corros. Sci.*, 10(1970), p.245.

[12] K. Darowicki, S. Krakowiak, and P. Ślepski, Evaluation of pitting corrosion by means of dynamic electrochemical impedance spectroscopy, *Electrochim. Acta*, 49(2004), No.17-18, p.2909.

[13] M.M. El-Naggar, Cyclic voltammetric studies of carbon steel in deaerated $NaHCO_3$ solution, *J. Appl. Electrochem*., 34(2004), p.911.

[14] D.D. Macdonald and M.C.H. McKubre, Corrosion of materials, [in] *Impedance Spectroscopy Emphasizing Solid Materials and Systems*, John Wiley & Sons, New York, 1987, p.260.

[15] D.G. Li, Y.R. Feng, Z.Q. Bai, *et al*. Photo-electrochemical analysis of passive film formed on X80 pipeline steel in bicarbonate/carbonate buffer solution, *Appl. Surf. Sci*., 254(2008), p.2837.